Charge radii and leptonic decay constants of heavy–light mesons in a potential model

Tapashi Das, D K Choudhury, K K Pathak & N S Bordoloi

Indian Journal of Physics

ISSN 0973-1458
Volume 95
Number 5

Indian J Phys (2021) 95:967-980
DOI 10.1007/s12648-020-01769-5

Springer

Indian J Phys (May 2021) 95(5):967–980
https://doi.org/10.1007/s12648-020-01769-5

ORIGINAL PAPER

Charge radii and leptonic decay constants of heavy–light mesons in a potential model

T Das[1]*, D K Choudhury[2], K K Pathak[3] and N S Bordoloi[4]

[1]Department of Physics, Madhab Choudhury College, Barpeta 781301, India

[2]Department of Physics, Gauhati University, Guwahati 781014, India

[3]Department of Physics, Arya Vidyapeeth College, Guwahati 781016, India

[4]Department of Physics, Cotton University, Guwahati 781001, India

Received: 17 June 2019 / Accepted: 06 January 2020 / Published online: 3 July 2020

Abstract: We report the results for charge radii and decay constants of heavy–light D and B mesons in an improved QCD potential model. To enhance the effectiveness of short-range and long-range effect of the potential $V(r) = -\frac{4\alpha_s}{3r} + \mathrm{br}$ in the perturbative procedure a cutoff parameter r^P is introduced as an integration limit. Another cutoff r_0 is used for the polynomial approximation of the series expansion used in the Dalgarno's method of perturbation. The results obtained are found to be in agreement with other available data. The limitation of the approach is discussed in the manuscript.

Keywords: Quantum chromodynamics; Dalgarno's method; Form factor; Charge radius; Decay constant

1. Introduction

The potential model description in the non-relativistic regime of QCD [1] is found to be very successful for both qualitative and quantitative descriptions of hadron spectroscopy.

The Coulomb plus linear Cornell potential [2], $V(r) = -\frac{4\alpha_s}{3r} + \mathrm{br} + c$, is very useful to apply in the quantum mechanical perturbation theory in the study of heavy-flavored mesons. At short distance, linear term is effectively considered as perturbation, while at long distance Coulomb potential is considered as perturbation. Hence this potential is based on the two kinds of asymptotic behaviors: ultraviolet at short distance (Coulomb like) and infrared at large distance (linear confinement term). In the Cornell potential, $-\frac{4}{3}$ is due to the color factor, α_s is the strong coupling constant, r is the inter-quark distance, b is the confinement parameter, and 'c' is a constant scale factor which is a phenomenological constant and is introduced basically to reproduce correct masses of heavy–light meson bound state.

In the present work, we have considered the scaling factor $c = 0$ as is done in Ref. [3–5]. For the Cornell potential, a constant term 'c' should not affect the wave function of the system while applying the perturbation theory. In Ref. [4], while applying the Dalgarno's method of perturbation [6, 7] it is seen that the term 'c' always appears in the total wave function. This is inconsistent with the quantum mechanical idea that a constant term 'c' in the potential can at best shift the energy scale, but should not perturb the wave function. Thus, a Hamiltonian H with such a constant and another H' without it should give rise to the same wave functions.

In this work, we introduce a cutoff parameter r^P as an integration limit, since it is well known that at short distance Coulomb potential plays a more dominant role than the linear confinement of the potential and at large distance the confinement takes over the Coulomb effect. Therefore, the inter-quark separation 'r' can be roughly divided into two regions $0 < r < r^P$ for short distance and $r^P < r < r_0$ for long distance effectively, 'r^P' is the point where one of the potentials will dominate over the other. In such situation, confinement parameter (b) and the strong coupling parameter (α_s) can be considered as effective and appropriate small perturbative parameters. In this work we have tried to incorporate both the short-range and long-range

*Corresponding author, E-mail: t4tapashi@gmail.com

effect of the potential in the construction of the total wave function and then to compute the charge radii and decay constants (f_D,f_{Ds},f_B,f_{Bs} and f_{Bc}) of D and B mesons. Decay constant f_P of mesons is important, because once it is known one can obtain the corresponding Cabibbo–Kobayashi–Maskawa (CKM) matrix element.

The results for charge radii and decay constants of mesons in this work are compared with earlier work [8–10] and also with the prediction of other models [2, 11–13].

We also study the variation of the wave functions with inter-quark distance 'r.' The study of the wave functions of heavy-flavored mesons like D and B is important not only for studying the properties of strong interactions between heavy and light quarks but also for investigating the mechanism of heavy meson decays.

The paper is organized as: in Sect. 2, we outline the formalism where we have discussed the model and form factor, charge radii and decay constants. The regularized wave function at the origin is obtained in Sect. 2. In Sect. 3, we summarize the results and discussion. Section 4 contains conclusion. The paper also contains two appendices A and B.

2. Formalism

2.1. The model

The non-relativistic two body Schrodinger equation [7] is

$$H|\psi\rangle = (H_0 + H')|\psi\rangle = E|\psi\rangle, \tag{1}$$

so that the first-order perturbed eigenfunction $\psi^{(1)}$ and eigenenergy $W^{(1)}$ can be obtained using the relation

$$H_0\psi^{(1)} + H'\psi^{(0)} = W^{(0)}\psi^{(1)} + W^{(1)}\psi^{(0)}, \tag{2}$$

where

$$W^{(0)} = \left\langle \psi^{(0)}|H_0|\psi^{(0)}\right\rangle, \tag{3}$$

$$W^{(1)} = \left\langle \psi^{(0)}|H'|\psi^{(0)}\right\rangle. \tag{4}$$

We calculate the total wave function using Dalgarno's method [6, 7] of perturbation for the Cornell potential with $c = 0$,

$$V(r) = -\frac{4\alpha_s}{3r} + \mathrm{br}. \tag{5}$$

The two choices for parent and perturbed Hamiltonian are

choice-I: $H_0 = -\frac{\nabla^2}{2\mu} - \frac{4\alpha_s}{3r}$ as parent and $H' = \mathrm{br}$ as perturbation and

choice-II: $H_0 = -\frac{\nabla^2}{2\mu} + \mathrm{br}$ as parent and $H' = -\frac{4\alpha_s}{3r}$ as perturbation.

From choice-I and choice-II, we can find the bounds on r up to which both the choices are valid.

From choice-I,

$$|-\frac{4\alpha_s}{3r}| > |\mathrm{br}| \tag{6}$$

and from choice-II,

$$|\mathrm{br}| > |-\frac{4\alpha_s}{3r}|. \tag{7}$$

The inequalities in (6) and (7) will correspond to a particular point r, say r^P, where $r^P = \sqrt{\frac{4\alpha_s}{3b}}$ such that for the short distance, i.e., $r < r^P$ Coulomb part is dominant over the linear confinement term, and for long distance, i.e., $r > r^P$ linear part is dominant over the Coulombic term. Thus, the point r^P measures the distance at which the potential changes from being dominantly Coulombic $(r < r^P)$ to dominantly linear $(r > r^P)$. At potential level, the continuity at a particular point of r is quite clear as is evident from Fig. 1 of Ref. [2].

The total wave function for choice-I is

$$\psi_I^{total}(r) = \frac{N}{\sqrt{\pi a_0^3}}\left[1 - \frac{1}{2}\mu b a_0 r^2\right]\left(\frac{r}{a_0}\right)^{-\epsilon} e^{-\frac{r}{a_0}}, \tag{8}$$

where the normalization constant N is

$$N = \left[\int_0^{r^P} \frac{4r^2}{a_0^3}\left[1 - \frac{1}{2}\mu b a_0 r^2\right]^2\left(\frac{r}{a_0}\right)^{-2\epsilon} e^{-\frac{2r}{a_0}}\mathrm{d}r\right]^{-\frac{1}{2}} \tag{9}$$

and

$$a_0 = \left(\frac{4}{3}\mu\alpha_s\right)^{-1}, \tag{10}$$

$$\mu = \frac{m_i m_j}{m_i + m_j}, \tag{11}$$

m_i and m_j are the masses of the quark and antiquark, respectively, μ is the reduced mass of the mesons, and

$$\epsilon = 1 - \sqrt{1 - \left(\frac{4}{3}\alpha_s\right)^2} \tag{12}$$

is the correction for relativistic effect [7, 14] due to Dirac modification factor.

Similarly, the total wave function for choice-II is

$$\psi_{II}^{total}(r) = \frac{N'}{r}\left[1 + A_0 r^0 + A_1(r)r + A_2(r)r^2 + A_3(r)r^3 + A_4(r)r^4 + \ldots\right]A_i[\rho_1 r + \rho_0]\left(\frac{r}{a_0}\right)^{-\epsilon}, \tag{13}$$

where $A_i[r]$ is the Airy function [15] and N' is the normalization constant,

$$N' = \left[\int_{r^P}^{r_0} 4\pi\left[1 + A_0 r^0 + A_1(r)r + A_2(r)r^2 + A_3(r)r^3 + A_4(r)r^4 + \ldots\right]^2 (A_i[\rho_1 r + \rho_0])^2 \left(\frac{r}{a_0}\right)^{-2\epsilon} \mathrm{d}r\right]^{-\frac{1}{2}}. \tag{14}$$

Even though the Airy's function vanishes exponentially as $r \to \infty$ [15] and is normalizable too, the additional cutoff r_0 is used in the integration basically due to the polynomial approximation of the series expansion used in the Dalgarno's method of perturbation and is independent of the property of the Airy's function.

The coefficients A_0, A_1, A_2, A_3, A_4, etc., of the series solution as occurred in Dalgarno's method of perturbation [4], are the function of α_s, μ and b:

$$A_0 = 0, \tag{15}$$

$$A_1 = \frac{-2\mu\frac{4\alpha_s}{3}}{2\rho_1 k_1 + \rho_1^2 k_2}, \tag{16}$$

$$A_2 = \frac{-2\mu W^1}{2 + 4\rho_1 k_1 + \rho_1^2 k_2}, \tag{17}$$

$$A_3 = \frac{-2\mu W^0 A_1}{6 + 6\rho_1 k_1 + \rho_1^2 k_2}, \tag{18}$$

$$A_4 = \frac{-2\mu W^0 A_2 + 2\mu b A_1}{12 + 8\rho_1 k_1 + \rho_1^2 k_2} \tag{19}$$

and so on.

The parameters:

$$\rho_1 = (2\mu b)^{\frac{1}{3}}, \tag{20}$$

$$\rho_0 = -\left[\frac{3\pi(4n-1)}{8}\right]^{\frac{2}{3}} \tag{21}$$

(in our case n=1 for ground state),

$$k = \frac{0.355 - (0.258)\rho_0}{(0.258)\rho_1}, \tag{22}$$

$$k_1 = 1 + \frac{k}{r}, \tag{23}$$

$$k_2 = \frac{k^2}{r^2}, \tag{24}$$

$$W^1 = \int \psi^{(0)\star} H' \psi^{(0)} d\tau, \tag{25}$$

$$W^0 = \int \psi^{(0)\star} H_0 \psi^{(0)} d\tau. \tag{26}$$

It is to be noted that though the Airy's function of infinite terms occurred in the model is approximated up to some finite orders of r, but our numerical analysis indicates that the term with $O(r^1)$ is sufficient to obtain numerically stable results. Therefore, the simplified version of Eq. (13) is taken as

$$\psi_{II}^{total}(r) = \frac{N'}{r}\left[1 + A_0 r^0 + A_1(r)r\right] A_i[\rho_1 r + \rho_0]\left(\frac{r}{a_0}\right)^{-\epsilon}, \tag{27}$$

where

$$N' = \left[\int_{r^P}^{r_0} 4\pi\left[1 + A_0 r^0 + A_1(r)r\right]^2 (A_i[\rho_1 r + \rho_0])^2 \left(\frac{r}{a_0}\right)^{-2\epsilon} \mathrm{d}r\right]^{-\frac{1}{2}}. \tag{28}$$

2.2. Variation of total wave functions and probability density with r

Figure 1(a), (b) and (c) shows the graphical variation of wave function $\psi_I(r)$ (Eq. 8), $\psi_{II}(r)$ (Eq. 27) and $\psi_I(r) + \psi_{II}(r)$ with r, respectively, and Fig. 1(d) shows the variation of probability density $|\, r(\psi_I(r) + \psi_{II}(r))\,|^2$ with r for $D(c\bar{u}/c\bar{d})$ meson.

Similarly, Fig. 2(a), (b) and (c) shows the graphical variation of wave function $\psi_I(r)$ (Eq. 8), $\psi_{II}(r)$ (Eq. 27) and $\psi_I(r) + \psi_{II}(r)$ with r, respectively, and Fig. 1(d) shows the variation of probability density $|\, r(\psi_I(r) + \psi_{II}(r))\,|^2$ with r for $B(u\bar{b})$ meson.

The graphical representation of the wave functions as well as the radial probability density with r shows similar variation as that of hydrogen atom [16] except that the scaling factors, 'm' the reduced mass of hydrogen atom, 'a' the atomic Bohr's radius, 'α' the fine structure constant, are replaced by 'μ' the reduced mass of the meson, 'a_0' the QCD analog of Bohr's radius and 'α_s' the strong coupling constant, respectively.

The qualitative features of the heavy-flavored meson wave functions (Figs. 1 & 2) are similar to those of the model of Ref. [17].

2.3. Form factor and charge radii

The elastic charge form factor for a charged system of point quarks has Q^2 dependent form [18]

$$F(Q^2) = \sum_{i=1}^{2} \frac{e_i}{Q_i} \int_0^\infty 4\pi r\, |\, \psi(r)\,|^2 \sin(Q_i r)\mathrm{d}r, \tag{29}$$

where Q^2 is the four momentum transfer square and e_i is the charge of the ith quark/antiquark and

$$Q_i = \frac{\sum_{j\neq i} m_j Q}{\sum_{i=1}^{2} m_i}, \tag{30}$$

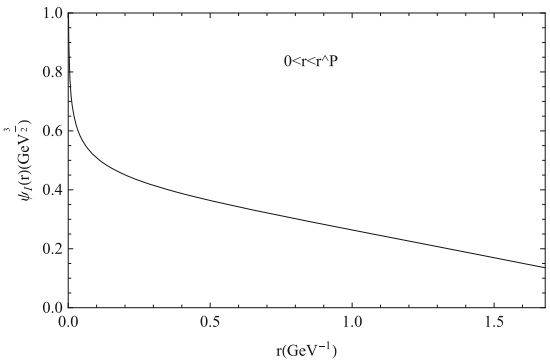

(a) Variation of radial wave function $\psi_I(r)$ with r.

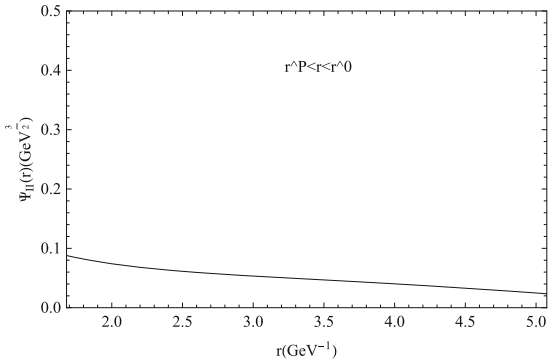

(b) Variation of radial wave function $\psi_{II}(r)$ with r.

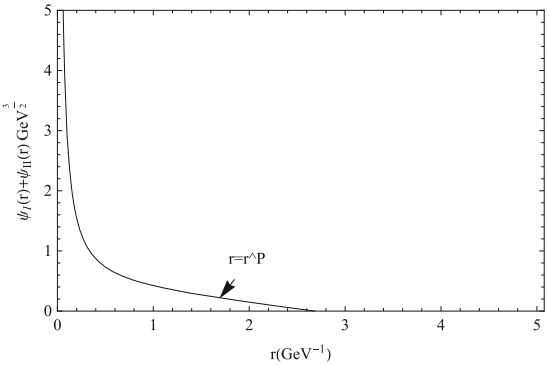

(c) Variation of wave function $\psi_I(r)+\psi_{II}(r)$ with r.

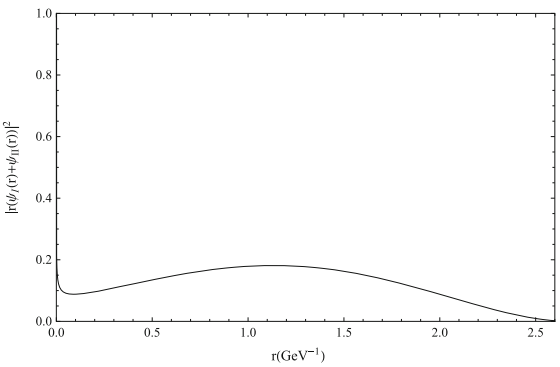

(d) Variation of radial probability density $\mid r(\psi_I(r)+\psi_{II}(r))\mid^2$ with r.

Fig. 1 Variation of $D(c\bar{u}/c\bar{d})$ meson wave function

where Q_i describes how the virtuality Q^2 is shared between the quark and antiquark pair of the meson.

In the present model, we redefine Eq. (29) as

$$F(Q^2) \approx \sum_{i=1}^{2} \frac{e_i}{Q_i} \int_0^{r^P} 4\pi r \mid \psi_I(r) \mid^2 \sin(Q_i r)\mathrm{d}r + \sum_{i=1}^{2} \frac{e_i}{Q_i} \int_{r^P}^{r_0} 4\pi r \mid \psi_{II}(r) \mid^2 \sin(Q_i r)\mathrm{d}r \tag{31}$$

$$F(Q^2) \approx F(Q^2) \mid_I + F(Q^2) \mid_{II} . \tag{32}$$

In Eqs. (31) and (32), we have used approximation signs rather than the equality sign because $F(Q^2) \mid_I$ will give approximate results for each form factor when $r \leq r^P$ and $F(Q^2) \mid_{II}$ will give approximate results when $r \geq r^P$.

To check the behavior of the form factor with momentum transfer square Q^2 we obtain the analytic expressions for form factors considering Airy's function up to order r^1 as shown in 'Appendices 1 and 2.'

$F(Q^2) \mid_I$ is solved using Coulomb potential as parent and linear potential as perturbation wave function (8) with relativistic correction (as shown in 'Appendix 1') which gives

$$F(Q^2) \mid_I \approx N^2 \sum_{i=1}^{2} e_i \left[\frac{1}{2^{1-2\epsilon}} \gamma(2-2\epsilon, r^P)(2-2\epsilon) \frac{1}{\left(1+\frac{a_0^2 Q_i^2}{4}\right)^{\frac{3}{2}-\epsilon}} - \frac{\mu b a_0^3}{2^{3-2\epsilon}} \gamma(4-2\epsilon, r^P)(4-2\epsilon) \frac{1}{\left(1+\frac{a_0^2 Q_i^2}{4}\right)^{\frac{5}{2}-\epsilon}} + \frac{\mu^2 b^2 a_0^6}{2^{7-2\epsilon}} \gamma(6-2\epsilon, r^P)(6-2\epsilon) \frac{1}{\left(1+\frac{a_0^2 Q_i^2}{4}\right)^{\frac{7}{2}-\epsilon}} \right], \tag{33}$$

where the incomplete gamma function $\gamma(s, r^P)$ is defined as

$$\int_0^{r^P} t^{s-1} e^{-t} dt = \gamma(s, r^P). \tag{34}$$

From the reality condition of Eq. (33), we obtain $0 < \epsilon < 1$; thus, form factor falls with the increasing value of Q^2.

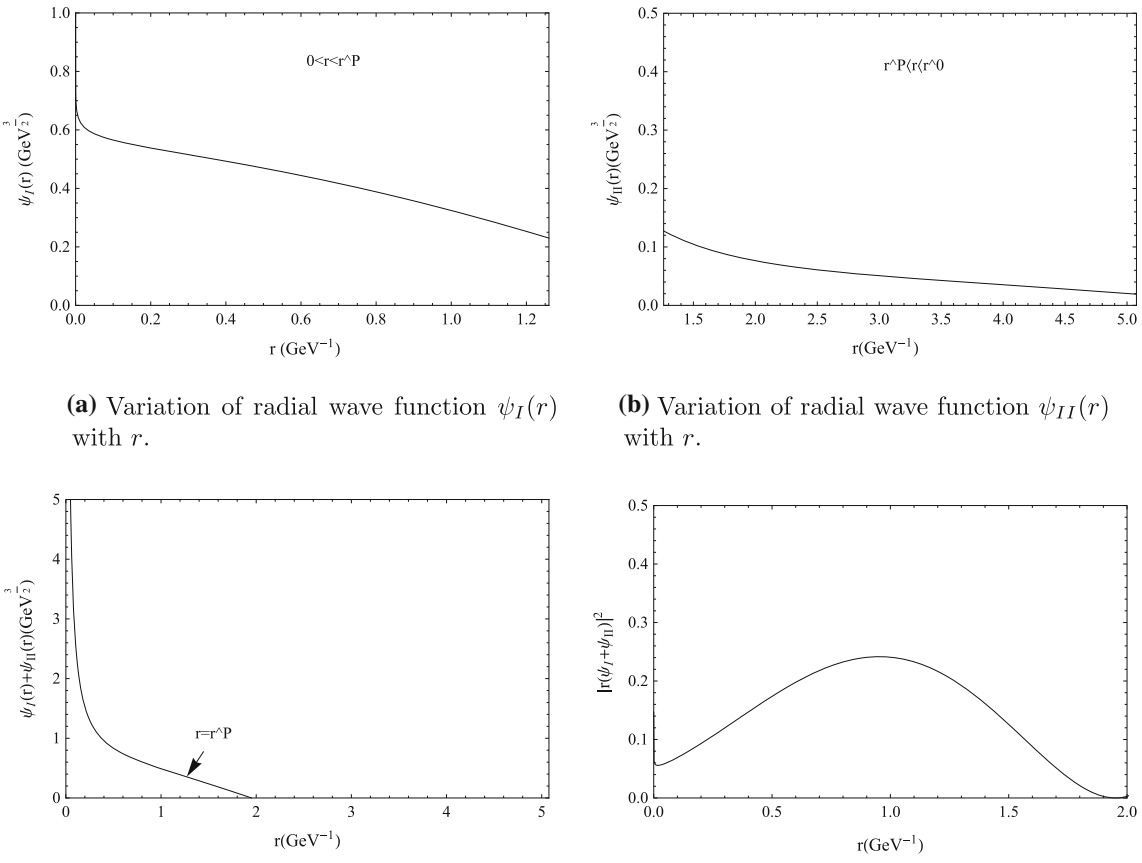

(a) Variation of radial wave function $\psi_I(r)$ with r.

(b) Variation of radial wave function $\psi_{II}(r)$ with r.

(c) Variation of wave function $\psi_I(r)+\psi_{II}(r)$ with r.

(d) Variation of radial probability density $|\, r(\psi_I(r)+\psi_{II}(r))\,|^2$ with r.

Fig. 2 Variation of $B(u\bar{b})$ meson wave function

Similarly, $F(Q^2)\,|_{II}$ is solved using wave function (27) (as shown in 'Appendix 2'), which gives

$$F(Q^2)\,|_{II} \approx 4\pi N'^2 a_0^{2\epsilon} \sum_{i=1}^{2} e_i \left[\sum_{k=1}^{11} F_k \frac{1}{(Q_i^2)^{\frac{k-2\epsilon}{2}}}\right], \tag{35}$$

where F_ks are defined in Eq. (63) of 'Appendix 2.'

The constraint on Eq. (35) is that for the term with $k = 1$, $\epsilon < 1$.

The average charge radii square for the mesons is extracted from the form factors at their low Q^2 behavior using the relation [11],

$$\begin{aligned}\langle r^2\rangle &= -6\frac{\mathrm{d}^2}{\mathrm{d}Q^2}F(Q^2)|_{Q^2=0} \\ &\approx -6\frac{\mathrm{d}^2}{\mathrm{d}Q^2}\left[F(Q^2)\,|_I + F(Q^2)\,|_{II}\right]|_{Q^2=0}.\end{aligned} \tag{36}$$

2.4. Decay constant in non-relativistic limit

In the non-relativistic limit, the pseudoscalar decay constant f_P and the ground state wave functions at the origin $\psi(0)$ are related by the Van–Royen–Weisskopf formula [19]

$$f_P = \sqrt{\frac{12}{M_P}|\psi(0)|^2}. \tag{37}$$

With QCD correction factor, the decay constant can be written as [20]

$$f_{P_c} = \sqrt{\frac{12}{M_P}|\psi(0)|^2 \bar{C}^2}, \tag{38}$$

where

$$\bar{C}^2 = 1 - \frac{\alpha_s}{\pi}\left[2 - \frac{m_i - m_j}{m_i + m_j} ln \frac{m_i}{m_j}\right], \tag{39}$$

where M_P is the pseudoscalar meson mass in the ground state that can be obtained as

$$M_P = m_i + m_j + \langle H\rangle, \tag{40}$$

where

$$\langle H\rangle = \left\langle \frac{p^2}{2\mu}\right\rangle + \langle V(r)\rangle. \tag{41}$$

The masses of the mesons obtained earlier in Ref.[5] are used in the present work.

Equations (37) and (38) show that we need to obtain wave function at the origin to find the decay constant. But with the Dirac modification factor $\left(\frac{r}{a_0}\right)^{-\epsilon}$, wave functions (8) and (13) at $r = 0$ develop a singularity. With $\epsilon = 0$, the wave function at the origin for (8) survives, but for (13) the singularity remains. In this case, one has to regularize the wave function at the origin [21] which has a quantum mechanical origin in QED. It is well known that the relativistic wave function of the hydrogen atom has such singularities too. However, such an effect is noticeable only for a tiny region [22],

$$2mz\alpha r \leq e^{-\left(\frac{1}{1-\gamma}\right)} \leq e^{-\frac{2}{z^2\alpha^2}} \sim 10^{-\frac{16300}{z^2}}, \tag{42}$$

where z and m are the atomic number and reduced mass of the hydrogen atom, respectively, α is the electromagnetic coupling constant and $\gamma = \sqrt{1 - z^2\alpha^2}$. In QCD, one replaces m, α and $(1 - \gamma)$, the hydrogen-like properties by $\mu, \frac{4}{3}\alpha_s$ and ϵ, respectively. Here α_s is the strong coupling constant, ϵ is as defined by Eq. (12) and $(2mz\alpha r)^{(\gamma-1)}$ changes to $\left(\frac{r}{a_0}\right)^{-\epsilon}$, which leads to a cutoff parameter 'r_c' up to which the model can be extrapolated $(r \geq r_c)$. Using the typical length scale for the relativistic correction term $\left(\frac{r}{a_0}\right)^{-\epsilon} \leq \frac{1}{e}$, one obtains

$$r_c \sim a_0 e^{-\frac{1}{\epsilon}}. \tag{43}$$

With this cutoff r_c, the normalized and regularized wave function corresponding to wave function (8) is

$$\psi_I^{total}(r') = \frac{N}{\sqrt{\pi a_0^3}}\left[1 - \frac{1}{2}\mu b a_0 (r')^2\right]\left(\frac{r'}{a_0}\right)^{-\epsilon} e^{-\frac{r'}{a_0}}. \tag{44}$$

Similarly, for (27), the corresponding regularized wave function is

$$\psi_{II}^{total}(r') = \frac{N'}{r}[1 + A_1 r']Ai[\rho_1 r' + \rho_0]\left(\frac{r'}{a_0}\right)^{-\epsilon}, \tag{45}$$

with

$$r' = r + r_c. \tag{46}$$

3. Results and discussion

The input parameters in the numerical calculations are $m_u = 0.336$ GeV, $m_s = 0.483$ GeV, $m_c = 1.55$ GeV, $m_b = 4.95$ GeV with $b = 0.183$ GeV^2 and α_s values 0.39 and 0.22 for charmonium and bottomonium scale, respectively, which are same as in the previous work [3–5, 23].

3.1. Values of r^P

In Table 1, we have recorded the numerical values of the cutoff parameter r^P in Fermi at charmonium and bottomonium scale.

3.2. Variation of form factor $F(Q^2)$ versus Q^2

With the same input parameters and setting the cutoff (r_0) in the range of 1 Fermi (5.076 GeV^{-1}) [24] for the wave function $\psi_{II}(r)$, in Fig. 3 we display the variation of form factor $F(Q^2)$ vs Q^2 for charged mesons ($D^+(c\bar{d})$, $D^+(c\bar{s})$ and $B^+(u\bar{b})$), and in Fig. 4 we display the variation of form factor for neutral mesons ($D^0(c\bar{u})$, $B^0(d\bar{b})$ and $B_s^0(s\bar{b})$), respectively, using Eq. (31).

From figures it can be concluded that the form factor of the charged mesons (Fig. 3) decreases with the increasing value of Q^2, but for neutral mesons (Fig. 4) form factor first increases for small Q^2 and then decreases with the increasing value of momentum transfer square. A similar behavior for neutral pseudoscalar Kaon is also suggested in Ref. [25]. The study shows a temporary rise in form factor does exist for heavy-flavored neutral mesons near $Q^2 \approx 1$ GeV^2 (Fig. 4). From the graphs as well as from Eq. (36) it is clearly seen that charge radii is negative for neutral mesons, since form factor is positive and hence the slope of the graph is positive.

3.3. Charge radii of mesons

In Table 2, we present our results for the charge radii for various D and B mesons using Eq. (36) and compare them with the results of Ref. [8, 9] and with the prediction of other models [11, 13].

From Table 2, we see that our results for $D^+(c\bar{d})$ and $D^0(c\bar{u})$ mesons are in good agreement with those of Ref. [13], but higher than those of Ref. [11]. In Ref. [9], the charge radii of various heavy and light mesons were found to be very small where Variationally Improved Perturbation Theory (VIPT) [2] was used. On the other hand, in Ref. [8], the charge radii of various mesons were calculated considering $b = 0$, where the results for heavy-flavored D mesons were found to agree well with the experimental values, but for heavy-flavored B mesons, the results were

Table 1 r^P in Fermi with $c = 0$ and $b = 0.183$ GeV^2

α_s value	r^P (Fermi)
0.39 (for charmonium scale)	0.332
0.22 (for bottomonium scale)	0.249

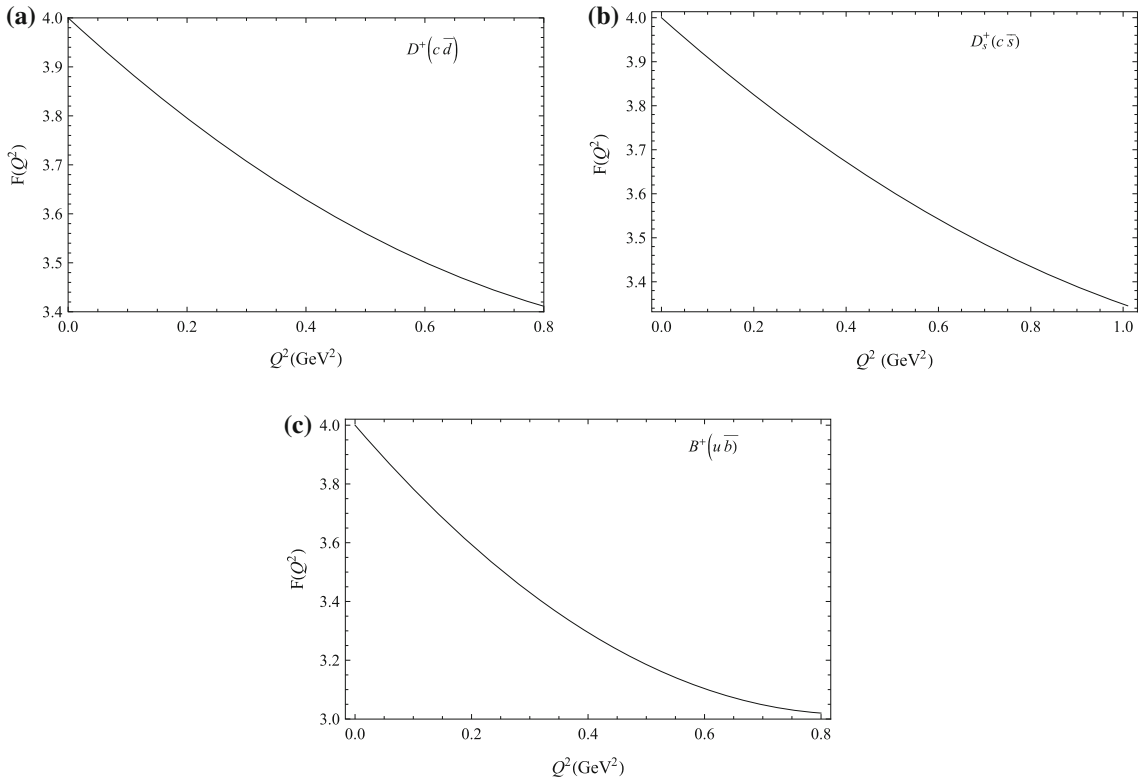

Fig. 3 Variation of form factor $F(Q^2)$ with Q^2 for **(a)** $D^+(c\bar{d})$ meson, **(b)** $D^+(c\bar{s})$ meson and **(c)** $B^+(u\bar{b})$ meson

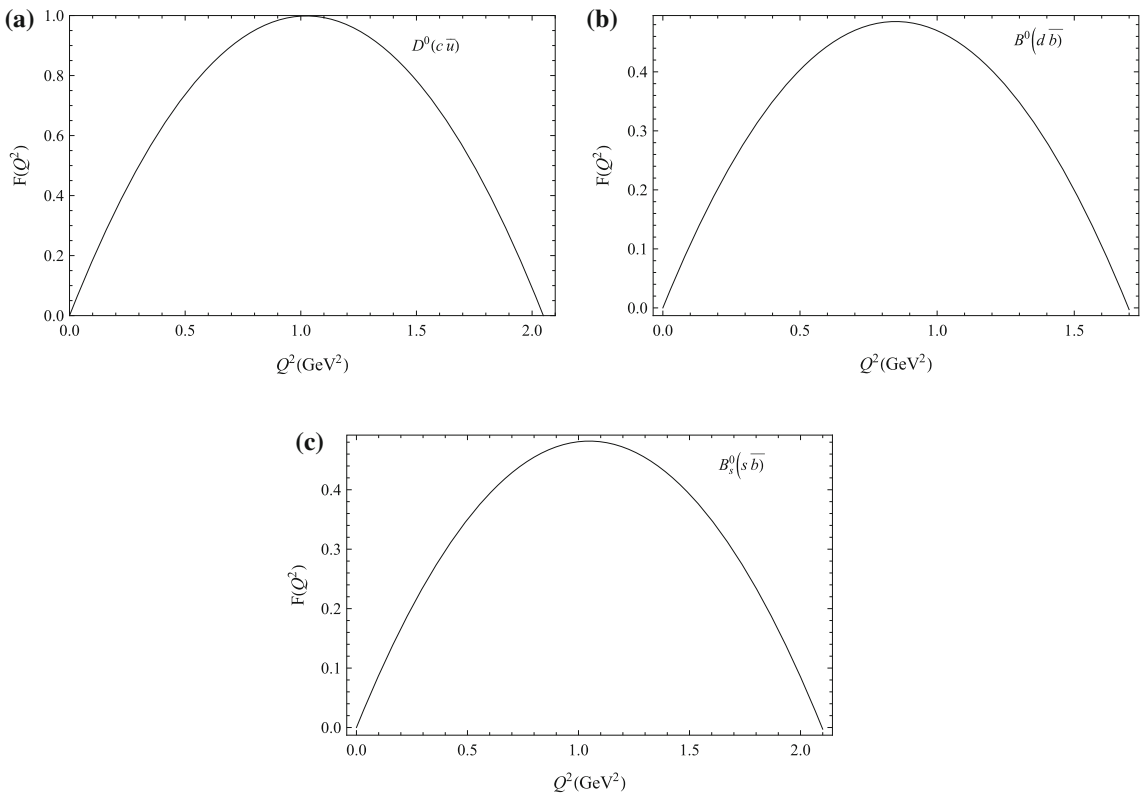

Fig. 4 Variation of form factor $F(Q^2)$ with Q^2 for **(a)** $D^0(c\bar{u})$, **(b)** $B^0(d\bar{b})$ and **(c)** $B_s^0(s\bar{b})$ meson

Table 2 The mean square charge radii of D and B mesons

Meson	$\langle r^2\rangle$ (Fermi^2)				
	Present work	Previous work[8]	Previous work [9]	[11]	[13]
$D^+(c\bar{d})$	0.260	0.134	0.011	0.184	0.219
$D^0(c\bar{u})$	− 0.453	− 0.234	− 0.013	− 0.304	− 0.403
$D_s^+(c\bar{s})$	0.216	0.126	0.010	0.124	–
$B^+(u\bar{b})$	0.536	2.96	0.060	0.378	–
$B^0(d\bar{b})$	− 0.266	− 1.47	− 0.030	− 0.187	–
$B_s^0(s\bar{b})$	− 0.214	− 1.37	− 0.025	− 0.119	–

large compared to other theoretical models. The present results for B mesons are found to be very much improved than the earlier analysis of Ref. [8, 9]. In Ref. [10], the charge radii of mesons were found for a nonzero value of scaling factor 'c' and with $b = 0.183$ GeV^2, where two-loop V-scheme was used for a large value of coupling constant $\alpha_v = 0.625$.

From Table 2, it is interesting to see that for all the neutral mesons the mean square charge radius is negative. A good explanation for negative charge radius square of the neutral meson can be found in Ref. [26]. Here let us explain this for neutral $D^0(c\bar{u})$ meson:

We define a center of mass coordinate for the quark antiquark $(Q\bar{q})$ bound state of meson,

$$R = \frac{m_Q r_Q + m_{\bar{q}} r_{\bar{q}}}{m_Q + m_{\bar{q}}}, \tag{47}$$

where r_Q and $r_{\bar{q}}$ are the heavy (Q) and light antiquark $(\bar{q})$ coordinates, respectively.

The mean square charge radius of the meson can be written as the deviation from the center of mass coordinate squared weighted by the quark and antiquark constituents of the meson, which has the simplified form,

$$\langle r^2\rangle_{D^0} = \frac{(Q_Q m_{\bar{q}}^2 + Q_{\bar{q}} m_Q^2)\langle\delta^2\rangle_{D^0}}{(m_Q + m_{\bar{q}})^2}, \tag{48}$$

where Q_Q and $Q_{\bar{q}}$ are charge of the quark and antiquark, respectively, and $\delta = (r_Q - r_{\bar{q}})$ is the relative coordinate.

For $D^0(c\bar{u})$ meson, $m_{\bar{q}} = m_{\bar{u}} = m = 0.336$ GeV
and $m_Q = m_c = 1.55$ GeV$= \gamma m$; $\gamma = 4.61$.
Thus from Eq. (48),

$$\langle r^2\rangle_{D^0} = \frac{2(1-\gamma^2)}{3(1+\gamma)^2}\langle\delta^2\rangle_{D^0}. \tag{49}$$

Since $\gamma = 4.61$ and $\langle\delta^2\rangle_{D^0} > 0$, from Eq. (49), it is clear that $D^0(c\bar{u})$ has a negative square charge radius.

In $D^0(c\bar{u})$ meson, a negatively charged light u-antiquark is orbiting around a heavier positively charged c-quark. Since the mass of c-quark is very large compared to the u-antiquark, when we probe lightly into the charge distribution, we will see the charge of the light objects which are in the tail of the distribution orbiting out at large distances.

The same explanation is valid for $B^0(d\bar{b})$ and $B_s^0(s\bar{b})$ mesons also, where a light d-quark is orbiting around a heavier b-antiquark and a light s-quark is orbiting around a heavier b-antiquark, respectively.

The perturbative stability of our results is also checked in the present model as shown in Table 3.

We have also checked the sensitivity of charge radii for different cutoff (r_0) values. The results are presented in Table 4.

From Table 4, it is seen that the higher value of the cutoff (r_0) raises the charge radii of the mesons. It is clear that our results for charge radii of mesons agree well with those of Ref. [11] when the upper cutoff r_0 will be between 0.689 and 0.788 Fermi. It is to be noted that the value of r_0 cannot be less than that of r^P.

3.4. Values of r_c

In Table 5, we compute the numerical values of small-scale r_c using (43) for various B and D mesons.

3.5. Decay constants using Van–Royen–Weisskopf formula

We calculate the decay constants of various D and B mesons using Eqs. (37) and (38) as shown in Table 6 with regularized wave functions (44) and (45).

Table 6 shows that the decay constant of mesons in coordinate space using Eq. (38) agrees well with the data. We also compare our results with lattice QCD results [29, 30, 32].

Table 3 Mean square charge radii of D and B mesons

Meson	$\langle r^2\rangle$ (Fermi^2)	
	With parent wave function	With total wave function
$D^+(c\bar{d})$	0.233	0.260
$D^0(c\bar{u})$	− 0.406	− 0.453
$D_s^+(c\bar{s})$	0.205	0.216
$B^+(u\bar{b})$	0.490	0.536
$B^0(d\bar{b})$	− 0.242	− 0.266
$B_s^0(s\bar{b})$	− 0.207	− 0.214

Table 5 Values of cutoff r_c in Fermi

Meson	r_c (Fermi)
$D(c\bar{u}/c\bar{d})$	0.00144
$D_s(c\bar{s})$	0.00108
$B(\bar{b}u/\bar{b}d)$	0.286×10^{-9}
$B_s(\bar{b}s)$	0.204×10^{-9}
$B_c(\bar{b}c)$	0.763×10^{-10}

4. Conclusion

In this work, we have first studied the charge radii of various heavy-flavored mesons $D^+(c\bar{d})$, $D^0(c\bar{u})$, $D_s^+(c\bar{s})$, $B^+(u\bar{b})$, $B^0(d\bar{b})$, $B_s^0(s\bar{b})$ in an improved version of a specific potential model [35] in which the short-range and long-range effect of the Cornell potential is expected to be enhanced in the perturbative procedure.

The scale parameter 'r^P' in the model is not an arbitrary parameter; rather, it depends on the strong coupling constant α_s and confinement parameter b. Again, we have used the same input parameters as is used in Ref. [3–5].

The charge radii of various heavy-flavored mesons have not been measured experimentally as yet. Our predicted results for charge radii of $D^+(c\bar{d})$ and $D^0(c\bar{u})$ mesons show good agreement with those of the model of Ref. [13]. From Table 4, it is clear that adjusting the upper cutoff r_0 to $\sim$0.788 Fermi, our results agree with those of Ref. [11]. In the present work, we have tried to explain the physical significance of negative charge radii of neutral mesons. The graphs of Fig. 4 show the variation of form factor $F(Q^2)$ with Q^2 for neutral mesons which indicate that the slope of the form factor is positive for Q^2 nearly up to 1 GeV^2.

On the other hand, the results for decay constants of mesons found using Eqs. (37) and (38) are well consistent with those of experimental data and other theoretical models.

Decay constants of heavy–light mesons (e.g., D, D_s mesons) are still not measured with high accuracy compared to light mesons (e.g., π, K mesons). However, the discrepancies are reduced to a certain extent by updates from experiments [28, 36–40]. Reliable experimental data for decay constants of D and D_s mesons have been obtained for measurements done in CLEO [28, 36, 37], Belle [38], BABAR [39], BES III [40] collaborations, etc. Again, the decay constant f_{B_s} for B_s meson cannot be measured experimentally due to its charge neutrality. Hence it has to be determined from theory. For experimentalists, it has now become a great challenge to extract the value of decay constant f_B of B meson.

In spite of its phenomenological success, the present version of the model has several inherent limitations. Let us therefore conclude with few comments:

(i) As noted in introduction, imposing an ad hoc assumption $c = 0$ in the potential removes the undesirable feature of the model at phenomenological level, but the model itself is not the way out to eliminate the possibility that one can measure the absolute value of the potential and not only the potential difference. However, the model with Variationally Improved Perturbation Theory (VIPT) [2] appears to remove this limitation. Here the r independent term (c) of the potential does not appear in the wave functions and hence in any observable.

Table 4 The sensitivity of mean square charge radii of D and B mesons with different r_0 values

Meson	$\langle r^2\rangle$ (Fermi^2)			
	$r_0 = 0.689$ Fermi	$r_0 = 0.788$ Fermi	$r_0 = 1$ Fermi	$r_0 = 1.379$ Fermi
$D^+(c\bar{d})$	0.166	0.200	0.260	0.307
$D^0(c\bar{u})$	− 0.289	− 0.349	− 0.453	− 0.535
$D_s^+(c\bar{s})$	0.152	0.180	0.216	0.305
$B^+(u\bar{b})$	0.337	0.410	0.536	0.617
$B^0(d\bar{b})$	0.167	− 0.204	− 0.266	− 0.306
$B_s^0(s\bar{b})$	− 0.167	− 0.180	− 0.214	− 0.287

Table 6 Decay constants of D and B mesons using Van–Royen–Weisskopf formula with regularized wave functions (44) and (45) and comparison with experimental data and other theoretical models

Meson	(This work) f_P	(This work) f_{P_c}	Experimental value & other work	Lattice QCD
D($c\bar{u}/c\bar{d}$)	0.293	0.274	0.205± 0.085±0.025 [27, 28] (Exp.)	0.220 ± 0.003 [29]
D_s ($c\bar{s}$)	0.368	0.335	0.254± 0.059 [27, 28] (Exp.)	0.258 ± 0.001 [30]
$B(\bar{b}u/\bar{b}d)$	0.206	0.203	0.207 ± 0.014 [17]	0.218 ± 0.005 [29]
			0.189 [31]	
B_s ($\bar{b}s$)	0.239	0.236	0.237± 0.017 [17]	0.228 ± 0.010 [32]
			0.218 [31]	
B_c ($\bar{b}c$)	0.410	0.389	0.433 (Rel), 0.562 (NR) [33]	-
			0.470 [34]	

All values are in the unit of GeV

(ii) The relativistic effects are incorporated directly by a multiplying factor $(\frac{r}{a_0})^{-\epsilon}$ in a free Dirac way, without other possible dynamics. Further study is needed to take into account such limitation.

Acknowledgements Most of the work was completed when one of the authors (T.Das) was completing her Ph.D thesis in the Department of Physics, Gauhati University. She gratefully acknowledges support given to her by the department. The authors also thank Dr Prakash Sharma, Principal, Madhab Choudhury College, Barpeta, for his kind support.

Appendix 1

With Coulomb parent linear perturbed wave function (8):

$$F(Q^2)\ |_I = \sum_{i=1}^{2} \frac{e_i}{Q_i} \int_0^{r^P} 4\pi r \mid \psi(r) \mid^2 sin(Q_i r) \mathrm{d}r \tag{50}$$

Using Eq. (8) in Eq. (50) and integrating over r,

$$\begin{aligned} F(Q^2)\ |_I = N^2 \sum_{i=1}^{2} \frac{e_i}{Q_i} \Bigg[& \frac{2^{2\epsilon}}{a_0} (\gamma(2-2\epsilon, r^P)) \sin((2-2\epsilon).\theta_i)(1+\frac{a_0^2 Q_i^2}{4})^{\epsilon-1} \\ & + \frac{a_0^5}{2^{6-2\epsilon}} \mu^2 b^2 (\gamma(6-2\epsilon, r^P)) \sin((6-2\epsilon).\theta_i)(1+\frac{a_0^2 Q_i^2}{4})^{\epsilon-3} \\ & - \frac{a_0^2}{2^{2-2\epsilon}} \mu b (\gamma(4-2\epsilon, r^P)) \sin((4-2\epsilon).\theta_i)(1+\frac{a_0^2 Q_i^2}{4})^{\epsilon-2} \Bigg] \end{aligned} \tag{51}$$

where

$$\theta_i = sin^{-1}\left[\frac{Q_i}{\left(Q_i^2 + \frac{4}{a_0^2}\right)^{\frac{1}{2}}} \right], \tag{52}$$

where only the first term of the following series is considered

$$sin^{-1}(x) \approx x + \frac{x^3}{6} + \frac{3x^5}{40}, \tag{53}$$

with

$$x = \frac{Q_i}{\left(Q_i^2 + \frac{4}{a_0^2}\right)^{\frac{1}{2}}} \tag{54}$$

which is true for very low Q^2.

We split the *sine* function of Eq. (51) using

$$sin(y) = y - \frac{y^3}{3!} + \frac{y^5}{5!}. \tag{55}$$

Now Eq. (51) becomes

$$\begin{aligned} F(Q^2)\ |_I = N^2 \sum_{i=1}^{2} \frac{e_i}{Q_i} \Bigg[& \frac{2^{2\epsilon}}{a_0} (\gamma(2-2\epsilon, r^P))((2-2\epsilon)\theta_i \\ & - \frac{(2-2\epsilon)^3}{3!}\theta_i^3 + \frac{(2-2\epsilon)^5}{5!}\theta_i^5 \Bigg) \left(1+\frac{a_0^2 Q_i^2}{4}\right)^{\epsilon-1} \\ & + \frac{a_0^5}{2^{6-2\epsilon}} \mu^2 b^2 (\gamma(6-2\epsilon, r^P)) \Bigg((6-2\epsilon)\theta_i - \frac{(6-2\epsilon)^3}{3!}\theta_i^3 \\ & + \frac{(6-2\epsilon)^5}{5!}\theta_i^5 \Bigg) \left(1+\frac{a_0^2 Q_i^2}{4}\right)^{\epsilon-3} \\ & - \frac{a_0^2}{2^{2-2\epsilon}} \mu b (\gamma(4-2\epsilon, r^P)) \Bigg((4-2\epsilon)\theta_i - \frac{(4-2\epsilon)^3}{3!}\theta_i^3 \\ & + \frac{(4-2\epsilon)^5}{5!}\theta_i^5 \Bigg) \left(1+\frac{a_0^2 Q_i^2}{4}\right)^{\epsilon-2} \Bigg]. \end{aligned} \tag{56}$$

Using (52) and (54) in the above equation,

$$F(Q^2)\mid_I = N^2 \sum_{i=1}^{2} e_i \left[\frac{2^{2\epsilon}}{a_0}(\gamma(2-2\epsilon, r^P))((2-2\epsilon)X_i - \frac{(2-2\epsilon)^3}{3!}Q_i^2X_i^3 + \frac{(2-2\epsilon)^5}{5!}Q_i^4X_i^5\right)(1+\frac{a_0^2Q_i^2}{4})^{\epsilon-1} + \frac{a_0^5}{2^{6-2\epsilon}}\mu^2b^2(\gamma(6-2\epsilon, r^P))((6-2\epsilon)X_i - \frac{(6-2\epsilon)^3}{3!}Q_i^2X_i^3 + \frac{(6-2\epsilon)^5}{5!}Q_i^4X_i^5\right)(1+\frac{a_0^2Q_i^2}{4})^{\epsilon-3} - \frac{a_0^2}{2^{2-2\epsilon}}\mu b(\gamma(4-2\epsilon, r^P))((4-2\epsilon)X_i - \frac{(4-2\epsilon)^3}{3!}Q_i^2X_i^3 + \frac{(4-2\epsilon)^5}{5!}Q_i^4X_i^5\right)(1+\frac{a_0^2Q_i^2}{4})^{\epsilon-2}\Bigg] \tag{57}$$

where

$$X_i = \left(Q_i^2 + \frac{4}{a_0^2}\right)^{-\frac{1}{2}}. \tag{58}$$

At low Q^2 limit, Eq. (57) reduces to Eq. (33).

$$F(Q^2)\mid_I = N^2 \sum_{i=1}^{2} e_i \left[\frac{1}{2^{1-2\epsilon}}(\gamma(2-2\epsilon, r^P))(2-2\epsilon)\left(1+\frac{a_0^2Q_i^2}{4}\right)^{\epsilon-\frac{3}{2}} - \frac{\mu b a_0^3}{2^{3-2\epsilon}}(\gamma(4-2\epsilon, r^P))(4-2\epsilon)\left(1+\frac{a_0^2Q_i^2}{4}\right)^{\epsilon-\frac{5}{2}} + \frac{\mu^2b^2a_0^6}{2^{7-2\epsilon}}(\gamma(6-2\epsilon, r^P))(6-2\epsilon)\left(1+\frac{a_0^2Q_i^2}{4}\right)^{\epsilon-\frac{7}{2}}\right]. \tag{59}$$

Appendix 2

With linear parent Coulomb perturbed wave function (27):

$$F(Q^2)\mid_{II} = \sum_{i=1}^{2}\frac{e_i}{Q_i}\int_{r^P}^{r_0} 4\pi r \mid \psi(r) \mid^2 \sin(Q_i r)\mathrm{d}r \tag{60}$$

Similarly, at low Q^2 limit Eq. (60) gives

$$
\begin{aligned}
F(Q^2)\ |_{II} = 4\pi N'^2 a_0^{2\epsilon} \sum_{i=1}^{2} e_i \Bigg[& \frac{(a_1 - b_1\rho_0)^2(\gamma(-2\epsilon, r_0) - \gamma(-2\epsilon, r^P))\sin((-2\epsilon)\phi_i)}{(Q_i^2)^{\frac{1-2\epsilon}{2}}} \\
& + \frac{(b_1\rho_1)^2(\gamma(2-2\epsilon, r_0) - \gamma(2-2\epsilon, r^P))\sin((2-2\epsilon)\phi_i)}{(Q_i^2)^{\frac{3-2\epsilon}{2}}} \\
& - \frac{2b_1\rho_1(a_1 - b_1\rho_0)(\gamma(1-2\epsilon, r_0) - \gamma(1-2\epsilon, r^P))\sin((1-2\epsilon)\phi_i)}{(Q_i^2)^{\frac{2-2\epsilon}{2}}} \\
& - \frac{16}{3}\frac{(a_1 - b_1\rho_0)^2\mu\alpha_s(\gamma(3-2\epsilon, r_0) - \gamma(3-2\epsilon, r^P))\sin((3-2\epsilon)\phi_i)}{(\rho_1 k)^2(Q_i^2)^{\frac{4-2\epsilon}{2}}} \\
& + \frac{16}{3}\frac{(a_1 - b_1\rho_0)^2\mu\alpha_s 2\sqrt{2\rho_1}(\gamma(4-2\epsilon, r_0) - \gamma(4-2\epsilon, r^P))\sin((4-2\epsilon)\phi_i)}{(\rho_1 k)^3(Q_i^2)^{\frac{5-2\epsilon}{2}}} \\
& - \frac{16}{3}\frac{(b_1\rho_1)^2\mu\alpha_s(\gamma(5-2\epsilon, r_0) - \gamma(5-2\epsilon, r^P))\sin((5-2\epsilon)\phi_i)}{(\rho_1 k)^2(Q_i^2)^{\frac{6-2\epsilon}{2}}} \\
& + \frac{16}{3}\frac{(b_1\rho_1)^2\mu\alpha_s 2\sqrt{2\rho_1}(\gamma(6-2\epsilon, r_0) - \gamma(6-2\epsilon, r^P))\sin((6-2\epsilon)\phi_i)}{(\rho_1 k)^3(Q_i^2)^{\frac{7-2\epsilon}{2}}} \\
& + \frac{32}{3}\frac{b_1\rho_1(a_1 - b_1\rho_0)\mu\alpha_s(\gamma(4-2\epsilon, r_0) - \gamma(4-2\epsilon, r^P))\sin((4-2\epsilon)\phi_i)}{(\rho_1 k)^2(Q_i^2)^{\frac{5-2\epsilon}{2}}} \\
& - \frac{32}{3}\frac{b_1\rho_1(a_1 - b_1\rho_0)2\sqrt{2\rho_1}\mu\alpha_s(\gamma(5-2\epsilon, r_0) - \gamma(5-2\epsilon, r^P))\sin((5-2\epsilon)\phi_i)}{(\rho_1 k)^3(Q_i^2)^{\frac{6-2\epsilon}{2}}} \\
& - \frac{8}{3}\frac{(a_1 - b_1\rho_0)^2\mu\alpha_s(\gamma(4-2\epsilon, r_0) - \gamma(4-2\epsilon, r^P))\sin((4-2\epsilon)\phi_i)}{(\rho_1 k)^2(Q_i^2)^{\frac{5-2\epsilon}{2}}} \\
& + \frac{8}{3}\frac{(a_1 - b_1\rho_0)^2\mu\alpha_s 2\sqrt{2\rho_1}(\gamma(5-2\epsilon, r_0) - \gamma(5-2\epsilon, r^P))\sin((5-2\epsilon)\phi_i)}{(\rho_1 k)^3(Q_i^2)^{\frac{6-2\epsilon}{2}}} \\
& + \left(\frac{8\mu\alpha_s}{3}\right)^2\frac{(b_1\rho_1)^2(\gamma(8-2\epsilon, r_0) - \gamma(8-2\epsilon, r^P))\sin((8-2\epsilon)\phi_i)}{(\rho_1 k)^4(Q_i^2)^{\frac{9-2\epsilon}{2}}} \\
& + \left(\frac{8\mu\alpha_s}{3}\right)^2\frac{8\rho_1(b_1\rho_1)^2(\gamma(10-2\epsilon, r_0) - \gamma(10-2\epsilon, r^P))\sin((10-2\epsilon)\phi_i)}{(\rho_1 k)^6(Q_i^2)^{\frac{11-2\epsilon}{2}}} \\
& - \left(\frac{8\mu\alpha_s}{3}\right)^2\frac{(b_1\rho_1)^2 4\sqrt{2\rho_1}(\gamma(9-2\epsilon, r_0) - \gamma(9-2\epsilon, r^P))\sin((9-2\epsilon)\phi_i)}{(\rho_1 k)^5(Q_i^2)^{\frac{10-2\epsilon}{2}}} \\
& - \left(\frac{8\mu\alpha_s}{3}\right)^2\frac{2b_1\rho_1(a_1 - b_1\rho_0)(\gamma(7-2\epsilon, r_0) - \gamma(7-2\epsilon, r^P))\sin((7-2\epsilon)\phi_i)}{(\rho_1 k)^4(Q_i^2)^{\frac{8-2\epsilon}{2}}} \\
& - \left(\frac{8\mu\alpha_s}{3}\right)^2\frac{2b_1\rho_1(a_1 - b_1\rho_0)8\rho_1(\gamma(9-2\epsilon, r_0) - \gamma(9-2\epsilon, r^P))\sin((9-2\epsilon)\phi_i)}{(\rho_1 k)^6(Q_i^2)^{\frac{10-2\epsilon}{2}}} \\
& + \left(\frac{8\mu\alpha_s}{3}\right)^2\frac{4b_1\rho_1(a_1 - b_1\rho_0)2\sqrt{2\rho_1}(\gamma(8-2\epsilon, r_0) - \gamma(8-2\epsilon, r^P))\sin((8-2\epsilon)\phi_i)}{(\rho_1 k)^5(Q_i^2)^{\frac{9-2\epsilon}{2}}} \Bigg],
\end{aligned}
\tag{61}
$$

where

$$\phi_i = \sin^{-1}(1),$$
$$a_1 = 0.355028,$$
$$b_1 = 0.258819,$$
$$b = 0.183\text{GeV}^2,$$
$$\rho_0 = -\frac{3}{4}3^{\frac{1}{3}}\pi^{\frac{2}{3}},$$
$$\rho_1 = 0.715309\mu^{\frac{1}{3}}$$
and $k = 1.33586\mu^{\frac{1}{3}}$.

Putting the above values in Eq. (61) and using approximations (53) and (55), Eq. (61) reduces to Eq. (62) which gives

$$F(Q^2)\,|_{II} = 4\pi N'^2 a_0^{2\epsilon}\sum_{i=1}^{2} e_i\left[F_1\frac{1}{(Q_i^2)^{\frac{1-2\epsilon}{2}}} + F_2\frac{1}{(Q_i^2)^{\frac{2-2\epsilon}{2}}} + F_3\frac{1}{(Q_i^2)^{\frac{3-2\epsilon}{2}}} + F_4\frac{1}{(Q_i^2)^{\frac{4-2\epsilon}{2}}} + F_5\frac{1}{(Q_i^2)^{\frac{5-2\epsilon}{2}}} + F_6\frac{1}{(Q_i^2)^{\frac{6-2\epsilon}{2}}} + F_7\frac{1}{(Q_i^2)^{\frac{7-2\epsilon}{2}}} + F_8\frac{1}{(Q_i^2)^{\frac{8-2\epsilon}{2}}} + F_9\frac{1}{(Q_i^2)^{\frac{9-2\epsilon}{2}}} + F_{10}\frac{1}{(Q_i^2)^{\frac{10-2\epsilon}{2}}} + F_{11}\frac{1}{(Q_i^2)^{\frac{11-2\epsilon}{2}}}\right], \tag{62}$$

where

$$F_1 = 0.913(\gamma(-2\epsilon, r_0) - \gamma(-2\epsilon, r^P))(-2\epsilon)$$
$$F_2 = -0.353\mu^{\frac{1}{3}}(\gamma(1-2\epsilon, r_0) - \gamma(1-2\epsilon, r^P))(1-2\epsilon)$$
$$F_3 = 0.0342\mu^{\frac{2}{3}}(\gamma(2-2\epsilon, r_0) - \gamma(2-2\epsilon, r^P))(2-2\epsilon)$$
$$F_4 = -5.33\mu\alpha_s(\gamma(3-2\epsilon, r_0) - \gamma(3-2\epsilon, r^P))(3-2\epsilon)$$
$$F_5 = (13.35\mu^{\frac{7}{6}} + 2.06\mu^{\frac{4}{3}} - 2.66\mu)\alpha_s(\gamma(4-2\epsilon, r_0) - \gamma(4-2\epsilon, r^P))(4-2\epsilon)$$
$$F_6 = (6.675\mu^{\frac{7}{6}} - 5.17\mu^{\frac{3}{2}} - 0.2\mu^{\frac{5}{3}})\alpha_s(\gamma(5-2\epsilon, r_0) - \gamma(5-2\epsilon, r^P))(5-2\epsilon)$$
$$F_7 = 0.501\mu^{\frac{11}{6}}\alpha_s(\gamma(6-2\epsilon, r_0) - \gamma(6-2\epsilon, r^P))(6-2\epsilon)$$
$$F_8 = -3.017\mu^{\frac{7}{3}}\alpha_s^2(\gamma(7-2\epsilon, r_0) - \gamma(7-2\epsilon, r^P))(7-2\epsilon)$$
$$F_9 = (0.292\mu^{\frac{8}{3}} + 15.1\mu^{\frac{5}{2}})\alpha_s^2(\gamma(8-2\epsilon, r_0) - \gamma(8-2\epsilon, r^P))(8-2\epsilon)$$
$$F_{10} = -(1.463\mu^{\frac{17}{6}} + 18.91\mu^{\frac{8}{3}})\alpha_s^2(\gamma(9-2\epsilon, r_0) - \gamma(9-2\epsilon, r^P))(9-2\epsilon)$$
$$F_{11} = 1.83\mu^3\alpha_s^2(\gamma(10-2\epsilon, r_0) - \gamma(10-2\epsilon, r^P))(10-2\epsilon). \tag{63}$$

We can express Eq. (62) as

$$F(Q^2)\,|_{II} = 4\pi N'^2 a_0^{2\epsilon}\sum_{i=1}^{2} e_i\left[\sum_{k=1}^{11} F_k\frac{1}{(Q_i^2)^{\frac{k-2\epsilon}{2}}}\right]. \tag{64}$$

In obtaining (59) and (64) we have also used the following integration

$$\int_0^\infty x^{p-1}e^{-ax}\sin(mx)\mathrm{d}x = \frac{\Gamma(p)\sin(p\theta)}{(a^2+m^2)^{\frac{p}{2}}}. \tag{65}$$

The following form of incomplete gamma function is used in obtaining (63)

$$\int_u^v t^{s-1}e^{-t}\mathrm{d}t = \gamma(s,v) - \gamma(s,u). \tag{66}$$

References

[1] F Halzen and A D Martin *Quarks and Leptons: An Introductory Course in Modern Particle Physics* (NewYork: Wiley), 205 (1984)
[2] I J R Aitchison and J J Dudek, *Eur. J. Phys.***23** 605 (2002)
[3] T Das and D K Choudhury, *Pramana J. Phys.***87** 52 (2016)
[4] T Das, D K Choudhury and K K Pathak, *Ind. J. Phys.***90** 1307 (2016)
[5] T Das, D K Choudhury and K K Pathak, *Int. J. Mod. Phys. A***31** 35 (2016)
[6] A Dalgarno *Stationary Perturbation Theory in Quantum theory I* (NewYork:Academic) D R Bates (1961)
[7] A K Ghatak and S Lokanathan, *Quantum Mechanics*, 5th edn. (McGraw Hill, 2004)
[8] N S Bordoloi and D K Choudhury, *Indian J. Phys.***82** 779 (2008)
[9] B J Hazarika and D K Choudhury, *Pramana J. Phys.***84** https://doi.org/10.1007/s12043-014-0839-x (2015)
[10] K K Pathak, N S Bordoloi and D K Choudhury, *Phys. Sci. Int.***7** 283 (2015)
[11] C W Hwang, *Eur. Phys. J. C***23** 585 (2002)
[12] F M Fernandez, *Eur. J. Phys.***24** 289 (2003)
[13] R J Lombard and J Mares, *Phys. Lett. B***472** 150 (2000)
[14] J J Sakurai, *Advanced Quantum Mechanics* (Massachusetts: Addison-Willey Publishing Company) 128 (1986)
[15] Abramowitz and Stegun, *Handbook of Mathematical Functions* (US: National Bureau of Standards) (10th ed), **46** (1964)
[16] F Schwabl, *Quantum Mechanics* (Narosa Publishing House, 1992)
[17] M Z Yang, *Eur. J. Phys. C***72** 1880 (2012)
[18] D P Stanley and D Robson, *Phys. Rev. D***21** 3180 (1980)
[19] R Van Royen *et al.*, *Nuovo Cimento***50** 617 (1967)
[20] E Braaten and S Fleming, *Phys. Rev. D***52** 181 (1995)
[21] K K Pathak, D K Choudhury, *Chin. Phys. Lett.***28** 10 (2011)
[22] C Itzykson and J Zuber, *Quantum Field Theory* (Singapore: International Student Edition, McGraw Hill), **79** (1986)
[23] K K Pathak and D K Choudhury, *Pramana J. Phys.***79** 6 (2012)
[24] G S Bali, *Proceedings from Quark Confinement and Hadron Spectrum IV*, (World Scientific, Ed. W. Lucha, K M Maung), p 209 (2002). https://doi.org/10.1142/9789812778567-0018. arXiv:hep-ph/0010032v1

[25] W I Giersche and C R Munz, *Phys. Rev. C***53** 5 (1996)
[26] D Green, *Lectures in Particle Physics* (World Scientific Notes in Physics) **55** 31
[27] D Asner et al. (Heavy Flavor Averaging Group). arXiv:1010.1589
[28] B I Eisenstein et al., (CLEO Collaboration) *Phys. Rev. D***78** 052003 (2008)
[29] E Eitchten et al., *Phys. Rev. D***21** 203 (1980)
[30] W Chen et al., TWQCD Collaboration, *Phys. Lett. B* 736 (2014)
[31] D Ebert, R N Faustov, V O Galkin, *Phys. Lett. B***635** 93. arXiv:0602110v2 [hep-ph] (2006)
[32] H Naetal, *Phys. Rev. D***86** 034506 (2012)
[33] D Ebert, R N Faustov and V O Galkin, *Phys. Rev. D***67** 014027 (2003)
[34] A K Rai, B Patel and P C Vinodkumar, *Phys. Rev. D***78** 055202 (2008)
[35] D K Choudhury et al., *Pramana J. Phys.***44** 519 (1995)
[36] K M Ecklund et al., (CLEO Collaboration) *Phys. Rev. Lett.***100** 161801 (2008)
[37] J P Alexander et al., (CLEO Collaboration) *Phys. Rev. D***79** 052001 (2009)
[38] K Abe et al., (Belle Collaboration) *Phys. Rev. Lett.***100** 241801 (2008)
[39] P del Amo Sanchez et al., (BABAR Collaboration) *Phys. Rev. D***82** 091103 (2010)
[40] R A Briere, (BES III Collaboration) arXiv:1308.1121v1 [hep-ex] (2013)